Materials Chemistry and Physics 135 (2012) 1084–1088

Contents lists available at SciVerse ScienceDirect

Materials Chemistry and Physics

journal homepage: www.elsevier.com/locate/matchemphys

Properties and phase composition of Ni–MgO–La_2O_3 systems submitted to different thermal treatments

Robson Santana Lima [a], Jadson Santos Moura [b], Genira Carneiro de Araújo [a], Viviana de Oliveira Mateus [a], Marluce Oliveira da Guarda Souza [a,*]

[a] Departamento de Ciências Exatas e da Terra, Universidade do Estado da Bahia, Campus I, Cabula 41, 195-001 Salvador, Bahia, Brazil
[b] Instituto de Química, Universidade Federal da Bahia, Campus Universitário de Ondina, Federação 40, 170-280 Salvador, Bahia, Brazil

HIGHLIGHTS

- ► $LaNiO_3$, Ni and $La_2O_2CO_3$ are formed to different thermal treatments of Ni–MgO–La_2O_3.
- ► The La/Mg = 1/1 and ½ ratios leads to a decline of peaks corresponding to perovskite.
- ► Mixed systems show a specific surface area higher than the nickel lanthanum system.
- ► Catalyst for application in hydrogen production reaction.

ARTICLE INFO

Article history:
Received 29 May 2011
Received in revised form
23 May 2012
Accepted 13 June 2012

Keywords:
Mixed system
Nickel Catalyst
Lantanum oxide
Magnesium oxide

ABSTRACT

This work investigated the properties and phase composition of nickel-based systems supported on mixed oxides of lanthanum and magnesium (in different proportions) that were submitted to different thermal treatments. Catalysts were obtained by co-precipitation and were characterised using different techniques. The diffractograms of the nickel and lanthanum oxide catalysts show more intense peaks associated with a perovskite-type phase. The presence of magnesium leads to a decrease in the intensity of the peaks that correspond to the perovskite phase. The mixed system showed a higher specific surface area compared with that of the system formed by nickel and lanthanum oxides. The specific surface area of the mixed system was proportional to the magnesium content. The reduction profiles showed interactions in these systems. Metallic nickel is formed at temperatures greater than 873 K after reduction with hydrogen. The $La_2O_2CO_3$ phase is formed under hydrogen-production reaction conditions. In conclusion, the systems formed by nickel, lanthanum and magnesium exhibit properties that render them suitable for application in hydrogen production reactions.

1. Introduction

Lanthanum oxide has diverse applications such as in the ceramic industry, in the manufacture of semiconductors and in various industries as catalyst supports [1–3].

The literature contains several studies related to the use of lanthanum oxide in nickel-based catalytic systems in several reactions for the generation of hydrogen, including the ethanol steam reforming reaction using hydrocarbon steam, the partial oxidation of natural gas and the reformation of methane using carbon dioxide. In diverse systems, lanthanum oxide is used as a catalytic support [4–6], as a dopant [7–9] and even in supports formed by mixed oxides [10].

A good example of the use of lanthanum oxide as a support is the nickel catalyst supported on lanthanum oxide (Ni/La_2O_3), which exhibits high stability during the ethanol steam reforming reaction. This stability may be explained by a mechanism based on a strong interaction of the lanthanum oxide with carbonaceous species [4,11]. The lanthanum oxide species that remain on the nickel react with the carbon dioxide from the reaction medium to form $La_2O_2CO_3$ [4].

The lanthanum oxicarbonate species react with the carbon in the metal surface, which circumvents an increase in the amount of coke and catalyst deactivation [4].

Lanthanum oxide shows a low specific surface area compared with other catalytic supports. The specific surface area of lanthanum oxide is approximately 20 $m^2\ g^{-1}$, which displays small variations according to the synthesis route of the material [9]. The

* Corresponding author.
E-mail addresses: mosouza@uneb.br, moguarda@gmail.com (M. Oliveira da Guarda Souza).

0254-0584/$ – see front matter © 2012 Elsevier B.V. All rights reserved.
http://dx.doi.org/10.1016/j.matchemphys.2012.06.021

commercial lanthanum oxides show a lower specific surface area of approximately 2 $m^2\ g^{-1}$ [12].

Magnesium oxide is another oxide that is primarily used as a catalytic support in diverse reactions; it contains defects in the crystalline net and provides optical, electronic and transport properties and superficial characteristics important for its application in catalysts [13–17].

Magnesium oxide is also used to form mixed supports in other matrixes, such as magnesium and aluminium obtained from the thermal decomposition of precursors with the hydrotalcite structure. Some studies of mixed oxides of lanthanum and magnesium obtained from mixtures of the respective oxides have been reported [18]. Systems based on Ni–MgO and Ni–La_2O_3 are known to form a solid solution ($Ni_{1-x}Mg_xO$) and a $LaNiO_3$ perovskite-type phase, respectively, after thermal decomposition of the precursors [19].

A previous study examined the thermal decomposition of precursors based on nickel (15% w/w), lanthanum and magnesium through variations in the La/Mg ratio [20]. The precursors were obtained by co-precipitation starting from solutions of metallic nitrates and using potassium carbonate or potassium hydroxide as the precipitant. This paper reports a study on the investigation of the catalysts based on nickel supported on mixed oxides of lanthanum and magnesium in different proportions. The catalysts were subjected to thermal treatment under reducing conditions, as well as exposure in a reformed ethanol steam to stimulate the hydrogen production.

2. Experimental

2.1. Catalyst preparation

The catalysts were prepared by co-precipitation from solutions of lanthanum, magnesium and nickel nitrates using solutions of potassium hydroxide and carbonate as precipitants to produce systems with 15% (w/w) nickel. The solutions were dosed using a peristaltic bomb (flux of approximately 0.7 mL min^{-1}). The temperature was maintained between 333 and 338 K, and the pH was controlled between 10 and 10.5. The gel formed was maintained under agitation for 2 h in the same temperature range. The material obtained was filtered and washed several times (using 1 L of water at 333 K) until the nitrate ions were completely removed.

The material was subsequently dried in a furnace (453 K, 24 h) and calcined by heating of the system from room temperature to 873 K at a heating rate of 10 K min^{-1}; the system was then maintained at 873 K for 2 h. The catalysts obtained were based on nickel supported on magnesium oxide, lanthanum oxide and mixed oxides of lanthanum and magnesium in the following proportions: La/Mg = 1, La/Mg = 2 and La/Mg = 1/2. The oxides of lanthanum and magnesium and the respective nickel catalysts were also obtained using only potassium hydroxide as the precipitant.

The obtained samples were identified as L, LM and M, which refer to lanthana, lanthana–magnesia and magnesia, respectively. 2LM and L2M refer to lanthana–magnesia samples with L/M atomic ratios of 2 and 0.5, respectively. NL, NM, NLM, 2NLM and N2LM refer to Ni-loaded lanthana–magnesia catalysts.

2.2. Characterisation

The metal contents were determined using X-ray dispersive spectroscopy. Pellets of all samples (obtained with a pellet press) were placed in a sample holder with double-sided carbon tape. The border of each pellet was subsequently wrapped with silvered ink, and the pellet was covered with carbon in a Battec MCS 010 metaliser to reduce static electricity. The EDX analyses were performed in a dispersive energy analyser of Si (Li) with beryllium windows (Oxford model 7060) at a resolution of 133 eV.

An SHIMADZU LAB-X XRD 6000 diffractometer was used in the X-ray diffraction experiments. The diffractometer was equipped with a nickel filter and a Cu Kα radiation ($\lambda = 1.54051$ Å) source. The tube power was 40 kV with a current of 30 mA and attenuation of 1000 cps. The slits used were divergent (1.0 mm), scattering (1.0) and reception (0.15 mm). The scanning velocity of the goniometer was 2° min^{-1} (2θ) over the 2θ range of 10–80°. All of the obtained diffractograms were compared with reference data sheets from the Joint Committee on Power Diffraction Standards (JCPDS) database.

The experiments to determine specific surface area were performed on a Micrometrics ASAP 2020. Approximately 0.25 g of the sample was treated at 473 K for 2 h in a vacuum of 6.6×10^4 Pa. The experiments related to physisorption were performed at 77 K. The programmed temperature reduction tests were performed in a Micrometrics Chemisorb 2720. Approximately 0.10 g of the sample was conditioned in a quartz cell and treated with nitrogen flux (30 mL min^{-1}) at increasing temperatures at a rate of 10 K min^{-1} until 473 K was reached; the sample was then maintained at 473 K for 2 h. After being pre-heated, the samples were cooled under nitrogen flux to room temperature; the samples were then warmed at a rate of 10 K min^{-1} from room temperature to 1273 K under a flux of a 5% H_2/N_2 mixture. The consumption of hydrogen was monitored using a thermal conductivity detector (TCD). In addition to these experiments, the catalyst reduction profile was analysed through reduction experiments performed on samples with hydrogen at temperatures of 673, 873 and 1073 K, followed by X-ray diffraction.

To verify the species formed under the hydrogen production conditions, the reaction samples were submitted to treatment in a reformed ethanol steam through the feeding of an ethanol/water solution (1:3 ratio, feeding flux of 2.5 mL h^{-1} and atmospheric pressure). The system was maintained at 873 K for 6 h.

3. Results and discussion

The results of chemical analyses show nickel contents and La/Mg ratios near those observed at the starting point.

The analysis of the X-ray diffraction results of the oxides without nickel (Fig. 1) reveals intense peaks in the lanthanum oxide diffractogram at 2θ angles of approximately 26° and 27°; these peaks are related to the presence of hexagonal-phase La_2O_3 [9]. Another

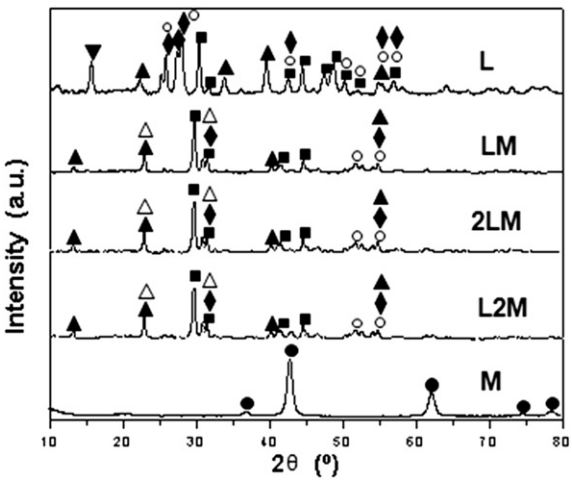

Fig. 1. X-ray diffractions of the supports. ■ LaOOH, ○ La_2O_3, ◆ $La_2O_2CO_3$, ▼ $La(OH)_3$, ▲ $La(NO_3)_3$, ● MgO, △ MgO_4, ▽ $Mg(OH)_2$, ◇ $MgO{\cdot}4NiO{\cdot}6O$.

high intensity peak observed at $2\theta = 30^\circ$ is characteristic of the LaOOH monoclinic phase [21]. The observed lower intensity diffraction lines are characteristic of the $La(OH)_3$ [22] phases as well as the nitrate and oxicarbonate species [23,24]. The oxicarbonate species result from the interaction of CO_2 (from the atmosphere) with the lanthanum oxide when carbonate was not used to precipitate the sample [25].

X-ray diffractograms of the mixed systems of lanthanum/magnesium show that the presence of magnesium leads to a diminished intensity of the peaks that correspond to lanthanum oxide, with the most intense peak corresponding to the LaOOH phase observed at a 2θ angle of approximately 29°. No profile modifications were observed with the lanthanum/magnesium ratio. The diffractogram of sample M is typical of magnesium oxide [18–26].

The diffractogram of sample NL shows a more intense peak at approximately 33°, which is associated with the formation of the perovskite-type $LaNiO_3$ phase [27]. The other peaks are characteristic of lanthanum oxide and the corresponding species of nitrates remaining from the synthesis reaction (Fig. 2).

Diffraction lines characteristic of oxicarbonate are also observed, and these lines are most likely from the interaction between atmospheric CO_2 and lanthanum oxide in samples where carbonate was not used to induce precipitation. The diffraction profiles of systems based on nickel and mixed oxides of lanthanum and magnesium showed diminished peak intensities that correspond to the perovskite phase in samples NLM and N2LM. No diffraction lines that correspond to the $LaNiO_3$ phase are observed when the magnesium content is increased (sample NL2M). These results indicate that the presence of magnesium inhibited the formation of perovskite, most likely due to the strong interaction between nickel oxides and magnesium.

The diffractogram of the NM catalyst shows that magnesium oxide, MgO, is the predominant phase, as indicated by the peaks at 2θ angles of 36°, 42°, 74° and 78°. The diffractogram of sample NM also shows simultaneous peaks of the MgO phase, which is characteristic of the formation of a magnesium and nickel solid solution ($Mg_{0.4}Ni_{0.6}O$) [18].

Table 1 shows the values of the specific surface areas measured using the BET technique. An increase in the specific surface area is observed to be proportional to the increase in the magnesium oxide content in each system. The presence of nickel reduced the specific surface area of the catalysts relative to the support areas. This effect is stronger in lanthanum oxide, most likely because of the formation of stable phases of perovskites between lanthanum and nickel during the calcining process; the formation of these phases results in a loss of surface area. The presence of perovskites was observed in the X-ray diffractograms of samples that contain nickel and lanthanum, except for the sample with the highest content of magnesium (NL2M), which showed the highest specific surface area among the systems.

Table 1
Specific surface areas of samples.

Sg BET			
Sample	($m^2\,g^{-1}$)	Sample	($m^2\,g^{-1}$)
L	24	NL	6
2LM	42	N2LM	21
LM	60	NLM	35
L2M	114	NL2M	47
M	194	NM	137

Fig. 3 shows the results of the temperature-programmed reduction (TPR). It is observed that the TPR of sample NL shows an initial peak at 661 K with the maximum consumption of hydrogen, which can be ascribed to the reduction of nickel species that minimally interact with the support, such as NiO that is amorphous to X-rays or to the first stage of perovskite reduction [18,25].

A second peak that is wider than the first (maximum at 807 K) may be associated with the last stage of perovskite reduction and with the reduction of the nickel species that strongly interact with defects in the lanthanum oxide structure [18]. The reduction profiles of the mixed oxides indicate that the presence of magnesium in the systems based on nickel and lanthanum makes the reduction process more difficult. This result can be explained by the strong MgO–NiO interaction [25].

In the system based on nickel and mixed oxides of lanthanum and magnesium with a La/Mg ratio of 1 (NLM), a first reduction peak is observed at 552 K, which may be associated with the reduction of NiO that is amorphous to X-rays and is finely dispersed on the support. Then, other peaks appear with maxima at temperatures of 703 and 781 K and a wider peak with a maximum at 894 K (Fig. 3). The appearance of these peaks indicates that nickel was dispersed throughout the whole oxide with different interactions in the different phases [18,25]. The first two peaks are associated with the process of perovskite reduction and with the reduction of nickel species that strongly interact with the defects in

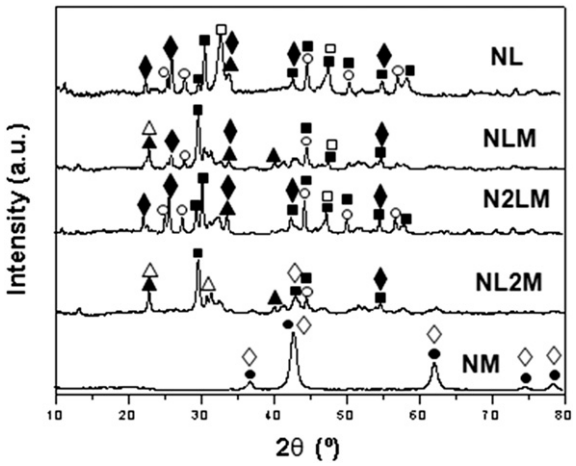

Fig. 2. X-ray diffractions of the catalysts. ◆ $La_2O_2CO_3$, ▼ $La(OH)_3$, ▲ $La(NO_3)_3$, ● MgO, △ MgO_4, ◇ MgO·4NiO·6O, □ $LaNiO_3$, ■ LaOOH, ○ La_2O_3.

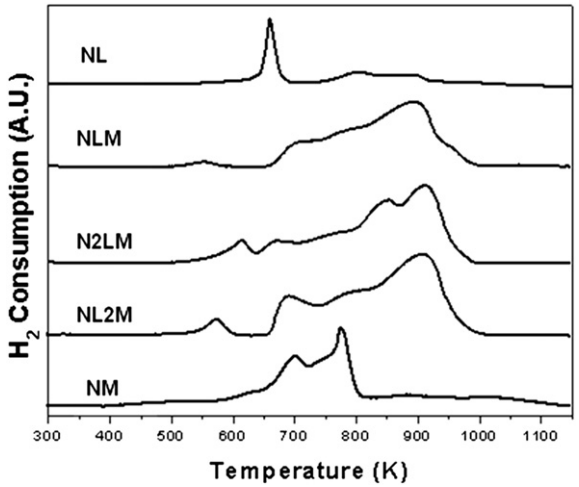

Fig. 3. Thermo programmed reduction of the catalysts.

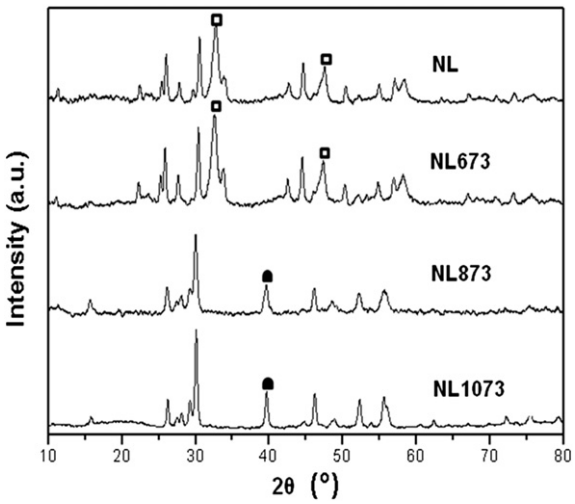

Fig. 4. X-ray diffractions of the catalysts based on nickel and lanthanum oxide (NL) reduced at the following temperatures: 673 K (NL 673), 873 K (NL 873) and 1073 K (NL 1073). ◘ Perovskite, ■ Metallic nickel.

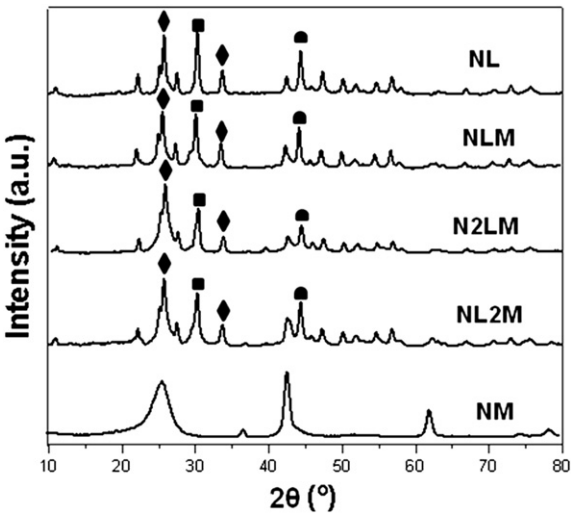

Fig. 6. XRD of the catalysts after reduction and thermal treatment in the ethanol reforming conditions. ■ LaOOH, ◆ $La_2O_2CO_3$ and ■ Metallic nickel.

the structure of lanthanum oxide [18,25]. The peak with a maximum at 894 K is associated with the reduction of species with stronger interactions with the system produced by the addition of magnesium [18]. These two events are recurrent in the thermograms of samples N2LMO and NL2MO, respectively. In the thermogram of sample N2LMO, the reduction peaks show maxima at 541, 676, 849 and 912 K. The values observed for sample NL2MO are 573, 690, 816 and 913 K (Fig. 3).

The thermogram of sample NM shows two reduction peaks at 704 and 777 K. Other lower peaks are observed at higher temperatures. In these systems, the process of reduction of the nickel species is more difficult due to the formation of the $Ni_{1-x}Mg_xO$ solid solution [18].

In addition to the temperature-programmed reduction experiments, other procedures were performed to evaluate the catalyst reduction processes. Initially, experiments with the nickel–lanthanum oxide system were performed by reducing samples with hydrogen at 673, 873 and 1073 K for 2 h with a constant flux of 5 mL min^{-1}. The resulting systems were analysed using XRD (Fig. 4).

Lines that correspond to metallic nickel were not observed in the diffractograms of sample NL673. The absence of a peak related to the nickel metallic phase in the diffractogram of sample NL673 is ascribed to the possibility of the species having small agglomerations with low crystallinity, which makes the identification by X-ray diffraction difficult. Nevertheless, the TPR results indicate that some nickel phases are reduced at higher temperatures. In fact, lines that correspond to metallic nickel at a 2θ angle of 40° (Fig. 4) were observed in the diffractograms of samples NL873 and NL1073. The peak that corresponds to the perovskite phase, which is present in the profiles of samples NL and NL673, was not observed in the diffractograms of samples NL873 and NL1073.

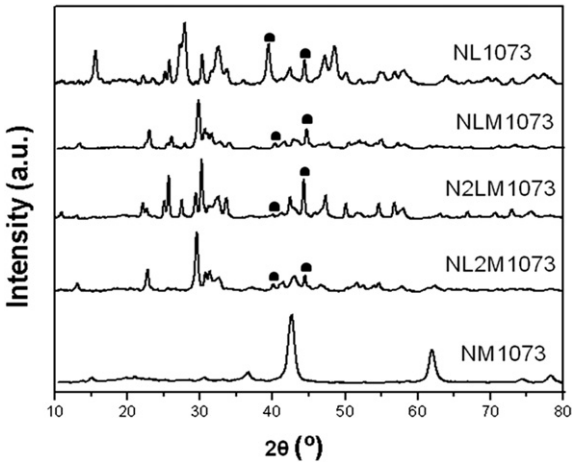

Fig. 5. X-ray diffractions of the catalysts reduced at 1073 K. ■ Metallic nickel

Because the reduction of sample NL occurred at different temperatures than those associated with the TPR results, the other samples were reduced with hydrogen at 1073 K for 2 h. The diffractograms are displayed in Fig. 5. The presence of a phase related to metallic nickel is observed, via the peaks at 2θ angles of 40° and 44°, in samples that contain lanthanum; the corresponding interplanar distances are 2.30 and 2.03, respectively [28]. The nickel support has a hexagonal-type crystalline structure. The peaks related to metallic nickel are more intense in mixed systems with higher lanthanum contents. In sample NM, a peak related to the metallic nickel phase was not identified, which suggests that NiO particles that are amorphous to X-rays on the magnesium oxide support are present and/or that nickel oxide particles that compose part of the solid solution were not reduced at this temperature [18].

The samples submitted to treatment under ethanol steam-reforming conditions were characterised using X-ray diffraction. Diffraction lines characteristic of the oxicarbonate and lanthanum phases were observed, with the most intense peak being ascribed to the $La_2O_2CO_3$ phase (Fig. 6). This result is in accordance with the observations of Fatsikostas et al. [4] with respect to the stability of the Ni/La_2O_3 catalyst, as the formation of coke is minimised by the formation of lanthanum oxicarbonate.

4. Conclusions

The catalyst based on nickel and mixed oxides of lanthanum and magnesium showed a higher specific surface area compared with that of the system formed by nickel and lanthanum oxides. The specific surface area of the mixed system was proportional to the magnesium content. The catalysts also exhibited diverse interactions, as shown by the reduction profiles. Metallic nickel is formed at temperatures greater than 873 K after reduction with hydrogen. Under ethanol-reforming conditions used for the production of hydrogen, the $La_2O_2CO_3$ phase is formed, and this phase

contributes to the stability of the catalyst. It is thus concluded that the systems formed by nickel, lanthanum and magnesium show properties that are suitable for application in hydrogen production reactions.

Acknowledgments

The authors wish to acknowledge the financial support received from CNPq (Conselho Nacional de Desenvolvimento Científico e Tecnológico) and Dr. Maria do Carmo Rangel, Dr. Artur José Santos Mascarenhas and Dr. Heloysa Martins de Andrade from GECCAT and LABCAT – UFBA (Universidade Federal da Bahia) for assistance with the analyses.

References

[1] L. Fornarini, J.C. Conde, P. S.ChiussiGonzalez, B. Leon, S. Martelli, Appl. Surf. Sci. 253 (2008) 7400–7405.
[2] A. Goel, D.U. Tulyaganov, V.V. Kharton, A.A. Yaremchenko, J.M.F. Ferreira, Elect. Acta Mater. 56 (13) (2008) 3065–3076.
[3] L. Shi, Y. Yuan, X.F. Liang, Y.D. Xia, J. Yin, Z.G. Liu, Appl. Surf. Sci. 253 (2007) 3731–3735.
[4] A.N. Fatsikostas, D.I. Kondarides, X.E. Verykios, Catal. Today 75 (2002) 145–155.
[5] D.K. Liguras, K. Goundani, X.E. Verykios, Int. J. Hydrogen Energy 29 (2004) 419–427.
[6] G.S. Gallego, F. Mondragón, J.-M. Tatibouët, J. Barrault, C. Batiot-Dupeyrat, Catal. Today 133–135 (2008) 200–209.
[7] M.C. Sánchez-Sánchez, R.M. Navarro, J.L.G. Fierro, Int. J. Hydrogen Energy 32 (2007) 1462–1471.
[8] Z. Xu, X. Zhong, J. Zhang, Y. Zhang, X. Cao, L. He, Surf. Coat. Technol. 202 (2008) 4714–4720.
[9] M.O.G. Souza, J.S. Moura, M.C. Rangel, Rev. Matér. 12 (2007) 29–38.
[10] J.A. Torres, J. Llorca, A. Casanovas, M. Domínguez, J. Salvadó, D. Montané, J. Power Sources 169 (2007) 158–166.
[11] A.S. Ivanova, Kinet. Catal. 46 (5) (2005) 620–633.
[12] E. Ruckenstein, Y.H. Hu, J. Catal. 161 (1996) 55–61.
[13] A. Tompos, M. Hegedűs, J.L. Margitfalvi, E.G. Szabó, L. Végvári, Appl. Catal. A 334 (1–2) (2008) 348–356.
[14] C. Trionfetti, I.V. Babich, K. Seshan, L. Lefferts, Langmuir 24 (2008) 8820–8828.
[15] M. Varga, Á Molnár, G. Mulas, M. Mohai, I. Bertóti, G. Cocco, J. Catal. 206 (2002) 71–81.
[16] K. Nagaoka, K. Sato, H. Nishiguchi, Y. Takita, Catal. Commun. 8 (2007) 1807–1810.
[17] E. Florez, P. Fuentealba, F. Mondragon, Catal. Today 133–135 (2008) 216–222.
[18] S.L. González-Cortés, I. Aray, S.M.A. Rodulfo-Baechler, C.A. Lugo, H.L. Del Castillo, A. Loaiza-Gil, F.E. Imbert, H. Figueroa, W. Pernía, A. Rodríguez, J. Mater. Sci. 42 (2007) 6532–6540.
[19] J.R. Rostrup-Nielsen, Catal. Today 63 (2000) 159–164.
[20] M.O.G. Souza, R.S. Lima, A.V. Santos, F.V. Pereira, J. Therm. Anal. Calorim. 100 (1) (2010) 83–87.
[21] JCPDS 77-2349.
[22] JCPDS 83-2034.
[23] JCPDS 77-1112.
[24] JCPDS 32-0490.
[25] J. Requies, M.A. Cabrero, V.L. Barrio, M.B. Guemez, J.F. Cambra, P.L. Arias, F.J. Perez-Alonso, M. Ojeda, M.A. Pena, J.L.G. Fierro, Appl. Catal. A 289 (2005) 214–223.
[26] JCPDS 78-0430.
[27] JCPDS 87-0217.
[28] JCPDS 45-1027.